ELSEVIER

Physica C 249 (1995) 187–195

PHYSICA C

A Monte Carlo study of proximity effects in electron-beam patterning of high-T_c superconducting thin films

Y.M. Gueorguiev *, K.G. Vutova, G.M. Mladenov

Institute of Electronics, Bulgarian Academy of Sciences, Tzarigradsko Shaussee 72, 1784 Sofia, Bulgaria

Received 20 February 1995; revised manuscript received 8 April 1995

Abstract

In the present work the proximity effects during the electron-beam lithography of $YBa_2Cu_3O_7$ high temperature superconducting thin films deposited on two typical substrates ($SrTiO_3$ and MgO) were studied at various beam voltages (25, 50, and 75 kV) by means of the Monte Carlo simulation. The radial distributions of the absorbed electron energy density obtained for all possible sets of initial conditions were approximated by an analytical function (namely a combination of a double Gaussian and an exponential function) and the parameters of this function were calculated. The distributions obtained in the present work as well as the calculated parameters of the so-called "proximity function" can be used in a proper proximity effect correction algorithm as well as in a profile development model.

1. Introduction

The reproducible fabrication of high temperature superconductor (HTS) electronic devices such as flux-flow transistors, sensors, superconducting quantum interference devices (SQUIDs), integrated circuits, microwave devices, etc. requires versatile lithographic and patterning processes allowing creation of submicron and even nanometer structures and not degrading the superconducting characteristics of the HTS thin films.

Several different technologies have been reported for the fabrication of submicron and nanometer patterns from HTS (mainly $YBa_2Cu_3O_7$) thin films, e.g. wet chemical etching [1–5], ion-beam and focused-ion-beam etching [6–10], reactive ion-beam etching [6,8,11], inhibit patterning [12–14], laser ablation [15–17] and ion implantation [6,18,19].

Most of these techniques are combined with electron-beam lithography (EBL), and moreover, until now best results are obtained by EBL in conjunction with wet chemical etching [4] as well as with ion-beam etching [7,10].

The high resolution of EBL however may be degraded by the lateral scattering of incident electrons which causes undesired exposure of unintended regions of the resist. This phenomenon is commonly referred to as "proximity effect" [21]. Electrons that are scattered during their first passage through the resist are called "forward scattered", while those which expose the resist after reaching the substrate are called "backscattered".

In the case of patterning the thin films of the most widely used HTS material, namely $YB_2C_3O_7$, de-

* Corresponding author.

SSDI 0921-4534(95)00287-1

posited on $SrTiO_3$, MgO, $ZrO_2:Y_2O_3$, $LaA10_3$, $NdGaO_3$, etc. substrates an enhanced proximity effect has to be taken into account because of their relatively high effective atomic numbers [9,20].

The proximity effect can be reduced technologically by using, if possible, thin resist films and membrane substrates, multilayer resist systems, or high accelerating voltage ($U_0 \geqslant 50$ kV). Another more widely used approach is to apply a proper proximity correction algorithm which adjusts the exposure dose and/or the shape and size of the exposed pattern. For realization of this approach and successful application of EBL a thorough understanding of electron scattering in solids as well as precise data for spatial distribution of the absorbed electron energy density in the resist are needed. This distribution describes quantitatively the proximity effect and is commonly approximated by an analytical function such as a double Gaussian [21–24]

$$f(r) = k\left[\exp(-r^2/\alpha^2)/\alpha^2 + \eta \exp(-r^2/\beta^2)/\beta^2\right]/\left[\pi(1+\eta)\right], \quad (1)$$

triple Gaussian [25,26]

$$f(r) = k\left[\exp(-r^2/\alpha^2)/\alpha^2 + \eta \exp(-r^2/\beta^2)/\beta^2 + \tau \exp(-r^2/\rho^2)/\rho^2\right]/\left[\pi(1+\eta+\tau)\right], \quad (2)$$

sixfold Gaussian [27]

$$f(r) = \sum_i A_i \exp(-r^2/\beta_i^2), \quad i = 1, 6, \quad (3)$$

and a combination of single or double Gaussians and exponential functions [28,29]

$$f(r) = k\left[\exp(-r^2/\alpha^2)/\alpha^2 + \eta \exp(-r^2/\beta^2)/\beta^2 + \nu \exp(-r/\gamma)/(2\gamma^2)\right] /\left[\pi(1+\eta+\nu)\right], \quad (4)$$

called "proximity function".

The parameters α, β, ρ, γ, η, τ, ν, and k of the proximity function can be evaluated both experimentally and theoretically. Experimental methods include: (i) measurements of exposed and developed finite shapes (e.g. rectangular cells, doughnut structures, etc.) [23,30–32]; (ii) measurements of single pass lines [24,26,]; (iii) measurements of point exposure distribution [28,33,34]. Theoretical methods include analytical [35–37] and computational (Monte Carlo simulation) models [29,34,38–41]. In spite of this large variety of methods for evaluation of the electron exposure distributions, Monte Carlo simulation (MCS) is the most widely used technique due to its advantages over other (especially experimental) methods [42].

The aim of the present work is to study the proximity effects at various beam voltages on typical targets incorporating $YBa_2Cu_3O_7$ HTS thin films by means of Monte Carlo simulation.

2. Theory

In this work a conventional Monte Carlo simulation based on both a single scattering model and a continuous slowing down approximation was used, assuming the screened Rutherford elastic scattering cross section and the Bethe energy loss equation. In order to prevent the failure of the latter one at low electron energies the parabolic extrapolation of the average energy loss rate $(dE/dx)^{-1}$ derived by Rao-Sahib and Wittry was introduced below a certain value of electron energy. In this way the incident electrons can be pursued until their energy decreases to 50 eV instead of the value of 500 eV which is commonly used as a cut-off energy.

Another peculiarity of the energy loss calculation is that instead of the conventional two-point difference scheme we involved the three-point difference scheme as proposed by Valiev et al. [44]. The application of the three-point difference scheme increases the accuracy of the energy loss calculation, especially at low beam energies as well as for heavy targets [45].

A procedure for recalculation of the free path length and of the energy loss of incident electrons at the inter-faces between different layers of the target was included in order to account for the differences in both the scattering and the stopping properties of their materials [43]. Such a procedure is particularly important in the case of targets incorporating

$YBa_2Cu_3O_7$ HTS thin films because of the relatively high differences in the values of effective atomic numbers and mass densities of target layers.

As usually in MCS of scattering of fast electrons in solids [29,34,38–41], we assume that the target layers are homogeneous in chemical composition and amorphous in structure. This assumption proved to yield good results especially for the calculation of energy loss distributions with regard to EBL. The presence of oxygen vacancies and precipitates in real HTS films may be taken into account in such a model by changing the stoichiometry and hence the concentration of the different atoms composing the film as well as its effective atomic number Z_{ef} and mass density ρ. Thus the influence of these defects onto the final results of the simulation depends on their amount. As to our knowledge in high quality films suitable for device fabrication this amount is not as great as to cause considerable changes of electron scattering.

For more details about the present Monte Carlo simulation model see, for instance, Refs. [20,29].

Radial distributions of the absorbed electron energy density in the resist obtained numerically for a zero-width δ-function were approximated by a combination of double Gaussian and exponential functions (Eq. (4)). The values of the parameters α, β, γ, η, ν, and k were calculated using an original Monte Carlo technique [46], instead of the commonly used non-linear least-squares method. This technique comprises the mean square deviation minimization by the interval length decrement for each of the parameters chosen. The minimization is made in an iteration loop.

The main advantages of the Monte Carlo technique described above are: (i) in contrast to some of the least-squares methods, it does not allow the possibility of an infinite loop in the case of a local minimum; (ii) it enables approximation of an arbitrary kind of distribution of numerical data with a corresponding analytical function.

3. Results and discussion

The present calculations were performed on an IBM 4381 machine. The radial distributions of the absorbed energy density were obtained for a zero-width δ-function with 30 000 electron trajectories for each simulation.

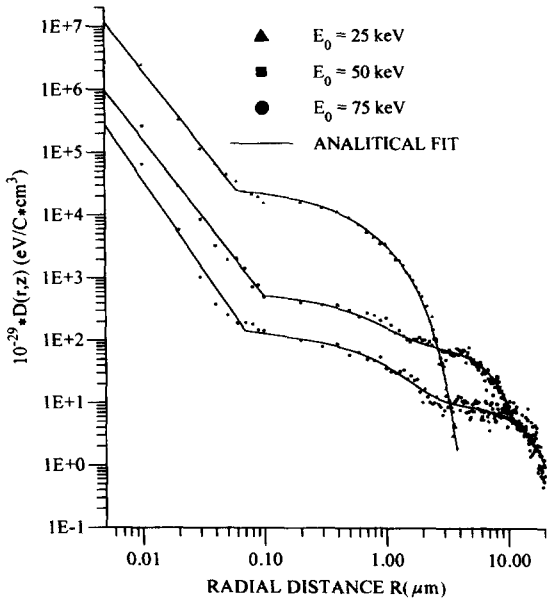

Fig. 1. Comparison between the exposure distributions obtained by MCS for the structure 125 nm PMMA resist film/300 nm $YBa_2Cu_3O_7$ HTS film/MgO substrate at three beam energies – 25, 50, and 75 keV and the corresponding analytical fits.

For the generation of random numbers the IBM uniform random number generator RNDM2 of the CERN Computer Centre Program Library was used. It is a combined multiplicative congruential generator and a shift register generator with a period of about 5×10^{18} numbers.

The variables studied in the present work are the substrate material ($SrTiO_3$ and MgO), the initial energy of accelerated electrons E_0 (25, 50 and 75 keV) and the HTS film thickness d (100 and 300 nm).

In Fig. 1 a comparison is made between the radial distributions of the absorbed energy density obtained by MCS for the structure 125 nm PMMA resist film/300 nm $YBa_2Cu_3O_7$ HTS film/MgO substrate at three beam energies, 25, 50, and 75 keV, and the corresponding analytical fits. It is well seen that the combination of double Gaussian and exponential functions is a good approximation of these distributions. Although not shown here, the double Gaussian as well as the triple Gaussian were also

tested but they were found to be not adequate, especially in the intermediate regions.

Figs. 2(a), 2(b), and 2(c) show the analytical fits to the radial distributions of absorbed energy density obtained by MCS for the structures 125 nm PMMA resist film/0, 100, or 300 nm $YBa_2Cu_3O_7$ HTS films/$SrTiO_3$ or MgO substrates at 25, 50, and 75 keV, respectively. Since the aim of the present work is to investigate the proximity effects caused by the YBCO film as well as by the substrate ($SrTiO_3$ or MgO) the backscattered exposure is of primary importance. For this reason here, in contrast to the Fig. 1, a linear scale for the x axis is applied which, although it compresses data points close to the beam

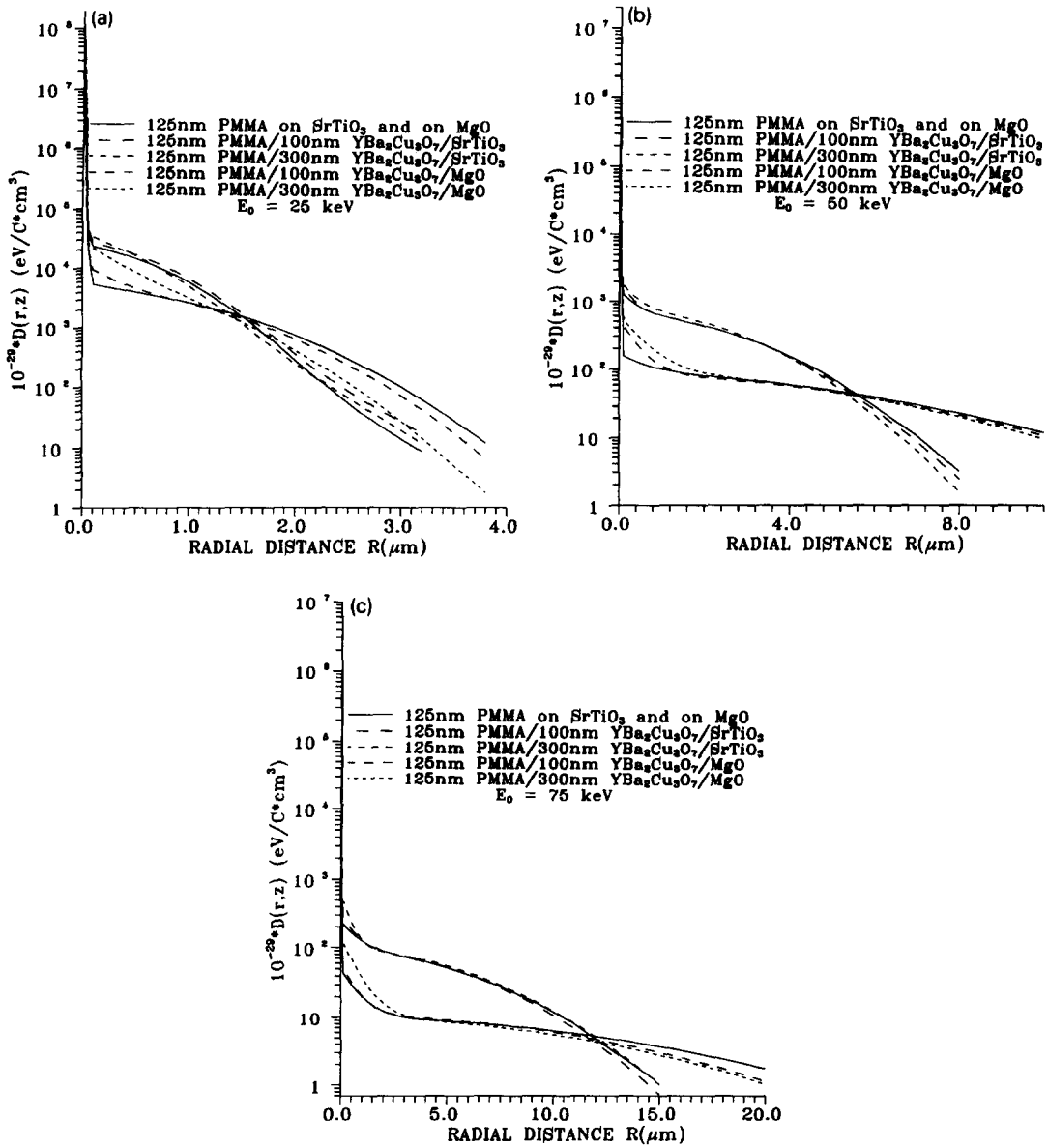

Fig. 2. Analytical fits of the exposure distributions in a 125 nm PMMA resist film on $SrTiO_3$ and MgO substrates as well as on 100 and 300 nm HTS layers of $YBa_2Cu_3O_7$ deposited on the substrates: (a) $E_0 = 25$ keV; (b) $E_0 = 50$ keV; (c) $E_0 = 75$ keV.

Table 1
List of the calculated values of the proximity function parameters for the $SrTiO_3$ substrate

E_0 (keV)	d (nm)	α (nm)	β (μm)	γ (μm)	η	ν	k
25	0	13.31	0.9398	0.4273	0.4834	0.1006	160033
	100	13.99	0.9322	0.4106	0.5689	0.2318	139967
	300	13.54	0.8562	0.3886	0.2470	0.3170	162456
50	0	12.25	3.5033	0.4022	0.9567	0.0321	50168
	100	12.78	3.4014	0.2573	0.9772	0.0373	41818
	300	13.20	3.2373	0.3880	0.8699	0.0628	48981
75	0	12.00	7.1568	0.7253	1.1561	0.0303	26995
	100	12.60	6.9217	0.4075	1.1725	0.0305	25034
	300	12.12	6.9110	0.4415	1.1070	0.0306	25935

axis (associated with the forward scattered electrons), it ensures a better distinction between the distributions in their intermediate and distant regions (associated with backscattered electrons).

In Tables 1 and 2 the calculated values of the proximity function parameters for $SrTiO_3$ and MgO substrates, respectively, are listed.

At the beginning of the discussion we would like to point out that when the exposure distributions are approximated by the combination of double Gaussian and exponential functions or by other complex analytical functions the division of scattering into forward and backward is not as definite as in the simplest cases of double Gaussian or the combination of single Gaussian and exponential functions. Nevertheless, we will use these terms for convenience.

The peaks of the distributions of the absorbed energy density are commonly attributed to the forward scattering of electrons or, in other words, to the single scattering of primary electrons into small angles in the resist. This scattering depends on the beam energy as well as on the material and thickness of the resist. In Figs. 1 and 2 it is seen that the maximum values as well as the widths of the peaks decrease with increasing beam energy. This can be explained by both the more efficient scattering of primary electrons and the higher energy loss in the resist at lower energies.

The parameter α of the proximity function is the width of the first Gaussian term in this function. It can be interpreted as a measure of the range of forward scattering of electrons. In Tables 1 and 2 it is seen that this parameter. decreases with increasing beam energy. Its higher values for the substrate of lower effective atomic number Z_{ef} and mass density ρ (i.e. MgO) are probably due to the wider spread of the distributions for this substrate, which influences the total results of the approximation.

We would like to note that the values of the parameter α listed here are calculated for a zero-width δ-function and are much smaller than the

Table 2
List of the calculated values of the proximity function parameters for the MgO substrate

E_0 (keV)	d (nm)	α (nm)	β (μm)	γ (μm)	η	ν	k
25	0	14.94	1.5649	0.3752	0.6926	0.0375	77244
	100	14.68	1.5113	0.2507	0.7980	0.1145	71486
	300	14.34	1.3528	0.3361	0.2644	0.2846	100820
50	0	12.98	6.9148	0.6980	1.0452	0.0221	25322
	100	13.40	6.7714	0.3157	1.1111	0.0379	20258
	300	13.20	6.6257	0.5699	0.7644	0.0939	25801
75	0	12.93	15.6316	0.7284	1.1201	0.0213	15213
	100	13.23	13.8983	0.6301	1.1479	0.0227	12687
	300	12.15	13.6265	0.6405	0.9890	0.0686	12632

beam size in most lithography machines. Therefore, the distributions given in Tables 1 and 2 should be convolved with the beam distribution of the concrete machine in order to obtain the actual distributions.

The parameter β is the width of the second Gaussian term in the proximity function. It is considered as an estimate of the range of electrons backscattered from the substrate to the resist as the result mainly of multiple scattering into small angles and, hence, of the range of the proximity effect. This parameter increases, as expected, with increasing beam energy as well as with decreasing the effective atomic number Z_{ef} and mass density ρ of the substrate material from $SrTiO_3$ to MgO. It is as lower as thicker is the HTS film. The latter can be explained as follows. The exposure of the resist in regions far from the point of incidence of the beam is caused by the electrons that have already undergone multiple scattering into small angles and have lost the main part of their energy in the substrate. A significant number of these electrons is absorbed in the HTS film and the number is as greater as thicker is the film. The features of the backscattered distributions discussed here can be seen in Figs. 1 and 2 as well.

The parameter η is the ratio of the exposure caused by the backscattered electrons associated with the second Gaussian term to that caused by the forward scattered electrons. It increases with increasing beam energy. The possible explanation of this fact is that although the levels of the backscattered distributions decrease as the beam energy increases, their widths increase significantly (see Fig. 1) so that the total exposure caused by the backscattered electrons increases too. It has to be added here that, as mentioned above, the maximum values of the forward scattering peaks are lower at higher accelerating voltages and this is another reason for the increase of η.

The values of the parameter η for the $SrTiO_3$ substrate are lower than those for the MgO substrate at 25 and 50 keV and this can be explained in the same way as for the variation of η with the beam energy. At 75 keV, however, the situation changes – the values of η for MgO substrate are slightly lower than those for the $SrTiO_3$ substrate. This fact shows that the widening of backscattered distributions for the MgO substrate at 75 keV are not sufficient to compensate for lowering of their levels so that the total backscattered exposure for the $SrTiO_3$ substrate becomes greater (see Fig. 2(c)).

The variation of η with the HTS film thickness is more complicated. The values of the parameter for all cases with $d = 100$ nm are higher than those with pure substrate ($d = 0$ nm). The possible reason for this fact is the additional contribution to the second Gaussian term of the electrons backscattered from the HTS film to the resist. For $d = 300$ nm the absorption in superconducting film of the electrons backscattered from the substrate dominates over the contribution of electrons backscattered from the HTS film so that the values of η are lower even than those for the pure substrate. It is worth pointing out that the variation of η with the HTS film thickness is more pronounced for the MgO substrate which means that the influence of this film upon the backscattered exposure of the resist is stronger for substrates of lower effective atomic number Z_{ef} and/or mass density ρ (see also Fig. 2).

It is necessary to note here that the higher values of the parameter η do not automatically mean a stronger proximity effect. As it was mentioned above, the total backscattered exposures at higher beam energies as well as for a lighter substrate (MgO) are higher but they are spreaded over wider areas. In the regions close to the incident point they are much lower and thus cause an almost uniform exposure background which could easily be compensated for using one uniform correction factor for all patterns to be exposed. Hence, the proximity effect at lower voltages as well as for heavy substrates is stronger, especially in dense patterns, and is more difficult to be compensated for.

Two kinds of electrons are considered to contribute to the exponential term of the proximity function which corresponds to the intermediate regions of exposure distributions. These are (i) the electrons backscattered from the HTS film to the resist layer and (ii) the electrons backscattered from the substrate to the resist mainly as the result of a single scattering into large angles. Both these kinds of electrons have lost a small part of their energy before reaching the resist layer again and a significant number of them leave the target as backscattered particles. Thus the mentioned electrons expose the resist only in areas close to the incident point of the beam.

The exponential term is described by the parameters γ and ν. The former one is the width of the term and is interpreted as a measure of the range of electrons contributing to the term. The latter one is the ratio of the exposure caused by these electrons to the forward scattered exposure.

In Tables 1 and 2 it is seen that the values of the parameter γ increase, as a whole, with increasing beam energy whereas the values of the parameter ν decrease. This is easy to understand – the electrons contributing to the exponential term are spreaded over longer lateral distances but their number is lower at higher accelerating voltages.

The values of γ for the MgO substrate are greater than those for the $SrTiO_3$ substrate which can be explained by the fact that a greater number of electrons are backscattered from the lighter substrate at lower angles (slightly greater than 90°) and they are spreaded over longer lateral distances. The values of ν for the $SrTiO_3$ substrate are greater than those for the MgO substrate for the pure substrate case ($d = 0$ nm) as well as for $d = 100$ nm, whereas for $d = 300$ nm they are smaller. This indicates the fact that the influence of the heavier substrate upon the exposure in the intermediate regions of the distributions is greater at lower HTS film thicknesses.

The values of the parameter ν increase significantly with increasing thickness of the HTS film. This fact shows that the electrons backscattered from the superconducting thin film are dominating contributors to the exponential term of the proximity function, especially for the lighter substrate as well as at lower beam energies. Besides, in Figs. 2(a), 2(b), and 2(c) it is well seen that the levels of the exposure distributions in intermediate regions are considerably higher for $d = 300$ nm even at 75 keV.

The variation of γ with the HTS film thickness is more complicated. The values of this parameter are greatest for the pure substrates and smallest for $d = 100$ nm. The possible explanation of this behavior is as follows. In the case of the pure substrates the exposure in intermediate regions is determined only by the electrons backscattered from the substrate and they may come out from significant depths within the substrate and be spreaded over longer lateral ranges. Thus they cause low level wide spreaded exposure (see (Figs. 2(a), 2(b), and 2(c)). When a superconducting film of thickness 100 nm is incorporated into the target it absorbs low energy wide spreaded electrons backscattered from the substrate. The number of electrons backscattered from the film itself is still not great and they are localized near the incident point because of its relatively low thickness. In the case of $d = 300$ nm the absorption of electrons coming from the substrate is more efficient but the backscattering within the HTS film is more efficient too. In this way a greater number of electrons are coming from the film to the resist and, besides, they are wider spreaded due to the greater thickness of the film and cause a high level exposure wider than in the case of $d = 100$ nm but still narrower than in the case of pure substrates.

The parameter k of the proximity function is a normalization parameter. Its value decreases together with the levels of the exposure distributions as the beam energy increases as well as the effective atomic number Z_{ef} and the mass density ρ of the substrate material decrease.

4. Conclusions

In this work the radial distributions of the absorbed electron energy density in a PMMA electron resist deposited on targets containing an $YBa_2Cu_3O_7$ HTS thin film were obtained by means of the Monte Carlo simulation for a zero-width δ-function and the following variables (i) the substrate material ($SrTiO_3$ and MgO), (ii) the electron beam energy E_0 (25, 50 and 75 keV), and (iii) the HTS film thickness d (0, 100, and 300 nm). These distributions stored as areas of numerical data were approximated by an analytical function, namely the combination of double Gaussian and exponential functions, which proved to be a good approximation to them. The values of the parameters of the analytical function were calculated using an original Monte Carlo technique, instead of the commonly used non-linear least-squares method, and their dependence on all investigated variables was discussed.

The results show that the additional backscattering of primary electrons and, hence, the proximity effect, caused by the HTS film in the regions close to the incident point of the electron beam are not completely eliminated even at energies as high as 75

keV, especially for the film thickness 300 nm as well as for the lighter substrate (MgO).

The HTS thin film reduces the backscattering from the underlying substrate and this reduction is as greater as thicker is the film as well as lower is the beam energy.

The distributions obtained in this work as well as the parameters of the proximity function can be employed in a proper proximity effect correction algorithm as well as in a resist development model.

Aknowledgements

This work was partially supported by the Bulgarian National Science Fund.

References

[1] J.A. Beall, M.W. Cromar, T.E. Harvey and M.E. Johansson, IEEE Trans. Magn. MAG-27 (1991) 1596.
[2] W.G. Lyons, R.R. Bonetti, A.E. Williams, P.M. Mankievich, M.L. O'Malley, J.J. Hamm, C. Anderson, R.S. Whiters and R.E. Howard, IEEE Trans. Magn. MAG-27 (1991) 2537.
[3] C.I.H. Ashby, J.S. Martens, T.A. Plut, D.S. Ginley and J.M. Phillips, Appl. Phys. Lett. 60 (1992) 2147.
[4] J.R. Wendt, J.S. Martens, C.I.H. Ashby, T.A. Plut, V.M. Hietala, C.P. Tigges, D.S. Ginley, M.P. Siegal, J.M. Phillips and G.K.G. Hohenwarter, Appl. Phys. Lett. 61 (1992) 1597.
[5] M.I. Faley, U. Poppe, H. Soltner, C.L. Jia, M. Siegel and K. Urban, Appl. Phys. Lett. 63 (1993) 2138.
[6] H. Tsuge, S. Matsui and N. Takado, IEEE Trans. Comp. Hybr. Manufact. Technol. 12 (1989) 548.
[7] R. Barth, B. Spangenberg, W. Langheinrich, W. Albrecht, H. Kurtz, G. Gieres and B. Holzapfel, J. Vac. Sci. Technol. A 10 (1992) 3411.
[8] L. Alff, G.M. Fischer, R. Gross, F. Kober, A. Beck, K.D. Husemann, T. Nissel, F. Schmidl and C. Burckhardt, Physica C 200 (1992) 277.
[9] W. Langheinrich, B. Spangenberg, R. Barth and H. Kurz, Microelectron. Eng. 21 (1993) 479.
[10] R. Barth, B. Spangenberg, C. Jaekel, H.G. Roskos, H. Kurz and B. Holzapfel, Appl. Phys. Lett. 63 (1993) 1149.
[11] S. Matsui, N. Nakano, H. Tsuge and K. Asakawa, Appl. Phys. Lett. 52 (1988) 69.
[12] Q.Y. Ma, E.S. Yang, G.V. Treys and C.-A. Chang, Appl. Phys. Lett. 55 (1989) 896.
[13] D.P. Kern, K.Y. Lee, R.B. Laibowitz and A. Gupta, J. Vac. Sci. Technol. B 9 (1991) 2875.
[14] C.A. Copetti, U. Gassig, W. Zander, J. Schubert and Ch. Buchal, Appl. Phys. Lett. 61 (1992) 3041.
[15] A. Inam, X.D. Wu, T. Venkatesan, S.B. Ogale, C.C. Chang and D. Dijkkamp, Appl. Phys. Lett. 51 (1987) 1112.
[16] J. Mannhart, M. Scheuermann, C.C. Tsuei, M.M. Oprysko, C.C. Chi, C. Umbach, R.H. Koch and C. Miller, Appl. Phys. Lett. 52 (1988) 1271.
[17] R.G. Humphreys, J.S. Satchell, N.G. Chew and J.A. Edwards, Appl. Phys. Lett. 54 (1989) 75.
[18] R.H. Koch, C. Umback, G.J. Clark, P. Chaudhari and R.B. Laibowitz, Appl. Phys. Lett. 51 (1987) 200.
[19] S. Matsui, Y. Ochiai, Y. Kojima, H. Tsuge, N. Takado, K. Asakawa, H. Matsutera, J. Fujita, T. Yoshitake and Y. Kubo, J. Vac. Sci. Technol. B 6 (1988) 600.
[20] J.M. Georgiev, G.M. Mladenov and D.I. Ivanov, Thin Solid Films 251 (1994) 67.
[21] T.H.P. Chang, J. Vac. Sci. Technol. 12 (1975) 1271.
[22] M. Parikh and D.F. Kyser, J. Appl. Phys. 50 (1979) 1104.
[23] R. Dimitrova, G. Mladenov and K. Vutova, Bulg. J. Phys. 14 (1987) 589.
[24] B. Dal'zotto, H. Dugourd, M. Lerme and F. Meot, Proc. of Microcircuits Engineering 1985, eds. K.D. van der Mast and S. Radelaar (North-Holland, Amsterdam, 1985) p. 105.
[25] S.J. Wind, M.G. Rosenfield, G. Pepper, W.W. Molzen and P.D. Gerber, J. Vac. Sci. Technol. B 7 (1989) 1507.
[26] C. Dix, P.G. Flavin, P. Hendy and M.E. Jones, J. Vac. Sci. Technol. B 3 (1985) 131.
[27] M.G. Rosenfield, S.A. Rishton, D.P. Kern, D.E. Seeger and C.A. Whiting, J. Vac. Sci. Technol. B 8 (1990) 1763.
[28] S.A. Rishton and D.P. Kern, J. Vac. Sci. Technol. B 5 (1987) 135.
[29] D.F. Kyser and K. Murata, IBM J. Res. Dev. 18 (1974) 352.
[30] W.D. Grobman and A.J. Speth, Proc. of the 8th Int. Conf. on Electron and Ion Beam Science and Technology, ed. R. Bakish (Electrochemical Society, Pennington, NJ, 1978) p. 276.
[31] V.V. Aristov, S.V. Babin, A.I. Erko and L.V. Dorozkina, Proc. of Microcircuit Engineering 1983 (Cambridge, UK, 1983) p. 57.
[32] W. Patrick and P Wettiger, J. Vac. Sci. Technol. B 3 (1985) 2037.
[33] C.P. Umbach and A.N. Broers, Appl. Phys. Lett. 56 (1990) 1594.
[34] M. Gentili, L. Grella, A. Lucchesini, L. Luciani, L. Mastrogiacomo and P. Musumeci, J. Vac. Sci. Technol. B 8 (1990) 1867.
[35] J.S. Greeneich and T. Van Duzer, IEEE Trans. Electron Devices ED-21 (1974) 286.
[36] R.J. Hawryluk, A.M. Hawryluk and H.I. Smith, J. Appl. Phys. 45 (1974) 2551.
[37] I. Raptis, N. Glezos and M. Hatzakis, J. Vac. Sci. Technol. B 11 (1993) 2754.
[38] K. Murata, D.F. Kyser and C.H. Ting, J. Appl. Phys. 52 (1981) 4396.
[39] K. Murata, H. Kawata, K. Nagami, Y. Hirai and Y. Mano, J. Vac. Sci. Technol. B 5 (1987) 124.
[40] S. Johnson and N.C. MacDonald, J. Vac. Sci. Technol. B 7 (1989) 1513.
[41] R. Shimizu and Z.-J. Ding, Rep. Prog. Phys. (1992) 487.

[42] Y. Gueorguiev, G. Mladenov and D. Ivanov, Proc. of the 4th Int. Conf. on Electron Beam Technology, June 6–11, 1994, Varna, Bulgaria (Sofia, Bulgaria, 1994) p. 315.
[43] J.M. Georgiev, Proc. of the 4th Int. Conf. on Electron Beam Technology, June 6–11, 1994, Varna, Bulgaria (Sofia, Bulgaria, 1994) p. 320.
[44] K.A. Valiev, A.N. Kirillov, B.N. Kovtun, T.N. Machviladze and M.M. Mkrtchian, Proc. of the Institute of General Physics at the Academy of Sciences of the USSR 8 (1987) 5 [in Russian].
[45] J. Georgiev, Proc. of the 8th International School Vacuum, Electron and Ion Technologies, September 26–October 1, 1993, Varna, Bulgaria, ed. D. Karpuzov (NOVA Science, USA, 1994) p. 406.
[46] K. Vutova and G. Mladenov, Modelling Simul. Mater. Sci. Eng. 2 (1994) 239.